data

MDPI

Data Descriptor

Indoor Temperature and Relative Humidity Dataset of Controlled and Uncontrolled Environments

Juan Botero-Valencia *,†, Luis Castano-Londono †and David Marquez-Viloria †

Faculty of Engineering, Instituto Tecnológico Metropolitano—ITM, Medellín 050034, Colombia; luiscastano@itm.edu.co (L.C.-L.); davidmarquez@itm.edu.co (D.M.-V.)

* Correspondence: juanbotero@itm.edu.co

† These authors contributed equally to this work.

Abstract: The large volume of data generated with the increasing development of Internet of Things applications has encouraged the development of a large number of works related to data management, wireless communication technologies, the deployment of sensor networks with limited resources, and energy consumption. Different types of new or well-known algorithms have been used for the processing and analysis of data acquired through sensor networks, algorithms for compression, filtering, calibration, analysis, or variables being common. In some cases, databases available on the network, public government databases, data generated from sensor networks deployed by the authors themselves, or values generated by simulation are used. In the case that the work approach is more related to the algorithm than to the characteristics of the sensor networks, these data source options may have some limitations such as the availability of databases, the time required for data acquisition, the need for the deployment of a real sensors network, and the reliability or characteristics of acquired data. The dataset in this article contains 4,164,267 values of timestamp, indoor temperature, and relative humidity acquired in the months of October and November 2019, with twelve temperature and humidity sensors Xiaomi Mijia at the laboratory of Control Systems and Robotics, and the De La Salle Museum of Natural Sciences, both of the Instituto Tecnológico Metropolitano, Medellín—Colombia. The devices were calibrated in a Metrology Laboratory accredited by the National Accreditation Body of Colombia (Organismo Nacional de Acreditación de Colombia—ONAC). The dataset is available in Mendeley Data repository.

Dataset: 10.17632/dxyvxk6h96.2

Keywords: temperature; relative humidity; Internet of Things (IoT); indoor climate

Citation: Botero-Valencia, J.; Castano-Londono, L.; Marquez-Viloria, D. Indoor Temperature and Relative Humidity Dataset of Controlled and Uncontrolled Environments. *Data* **2022**, *7*, 81. https://doi.org/10.3390/data7060081

Academic Editor: Joaquín Torres-Sospedra

Received: 7 May 2022
Accepted: 12 June 2022
Published: 16 June 2022

1. Introduction

The measurement of humidity and temperature helps us determine the system's behavior in a wide variety of applications. For this reason, these physical variables are among the most used in multiple applications in very different work areas, such as health [1,2], electronic circuits [3], precision agriculture [4], milk production [5], or climate change [6].

Within the measurements that we perform in the environment, there are two main fields: the outdoor [7], that is, the measurement that is performed outside any structure built by man, and the indoor [8,9] measurement, which is performed inside a building. Indoor measurement is an area that has attracted interest in recent years with the modernization of systems for indoor temperature control (cooling or heating) [10].

For example, in places where the temperature is not controlled and there is a continuous transit of people who inhabit the area, such as offices, gyms, event halls, or residential buildings, the works using temperature and humidity are focused on comfort studies [11–15]. In these places, the cooling or heating systems are turned on and off at the

convenience of the people living in the space, doors and windows can be opened, or computer equipment can be used with different computational intensities altering the internal microclimates and, therefore, the comfort of the people. In this work, the measurements were carried out in an office environment of the Control and Robotics Systems Laboratory, with doors and windows opened without control and with occasional air conditioning turned off.

In places where strict temperature and humidity control is needed, such as in food warehouses, research can be focused on understanding the microclimates produced by the heterogeneous distribution of air inside the warehouse [16]. There is usually no significant human intervention in temperature-controlled sites for long periods, maintaining a low temperature and humidity variation. The storage of museum pieces is also in temperature- and humidity-controlled spaces because these two physical variables strongly impact the deterioration of some museum pieces [17,18]. De La Salle Museum of Natural Science conserves an extensive collection of stuffed animals, insects, reptiles, birds, and mammals exhibited on a rotating basis in the different exhibition rooms of the museum. Still, they are preserved in humidity- and temperature-controlled storage most of the time. In this storage, the doors are opened for cleaning personnel and curators. The different storage shelves and the contact of museum walls with the outside of the building generate different microclimates. For this reason, this work can be interesting for researchers in indoor microclimates with controlled temperatures and humidity [19–21].

Many state-of-the-art studies use the Intel Berkeley Research Lab dataset [22] for the application of algorithms proposed to process data acquired with real-time wireless sensor networks (WSN). In these works, classical processing techniques are used as in [23,24], machine learning-based approaches as in [25–27], or both types of algorithms as in [28].

The dataset described in this article contains the information about the indoor temperature in °C and relative humidity in $\%RH$, acquired for two months with twelve Xiaomi Mijia sensors at the laboratory of Control Systems and Robotics, and the storage room of the De La Salle Museum of Natural Sciences, both of the Instituto Tecnológico Metropolitano, Medellín—Colombia. The devices used for the acquisition are low-cost and have a calibration certificate from a Metrology Laboratory accredited by the National Accreditation Body of Colombia (ONAC). This dataset provides the timestamp, the measured variables, and floor plans with the sensors distribution of the deployed WSN. In addition, the data description presented in this article provides additional information about the sensors, the deployed sensor network, and the sampling.

The installation of these sensor systems implies space adequacy, the researchers' knowledge of concepts of the Internet of Things (IoT), sensor networks, and embedded systems. Having data available to serve as a basis for researchers interested in digital signal processing and machine learning prevents them from deploying the sensor networks [29–31]. This work was chosen using wireless sensors using Bluetooth Low Energy (BLE) and a single gateway to read all sensors' temperature and humidity measurements [32–34]. This configuration avoids having an embedded system for each sensor to store the data and the need to have multiple power supply points. The setup presents the delays inherent to communication, i.e., there is no constant sampling period, but this is typical of IoT system implementations, where factors such as cost, energy savings, and reading multiple devices to a single gateway are crucial. The dataset presented in this work can contribute to studies on the behavior of sensor networks using BLE to develop techniques used in IoT [35,36].

For this work it is considered that the weather in Medellin, Colombia, has a negligible variation throughout the year and has no climatic seasons due to its location near the Equator. In this work, the measurement was performed for one month at each site, considering that the external weather factor in the city does not present significant changes. The set of sensors used is the same in the museum and the laboratory, so it was, therefore, necessary to acquire the data in two different months.

The paper is organized as follows. In Section 2, we present the acquisition devices, the description of the measurement area, and the description of the dataset organization. The

aspects related to the sampling and the analysis of some examples of the data acquired on specific dates in the laboratory and the museum are shown in Section 3. Finally, conclusions and future work are drawn in Section 4.

2. Materials and Methods

This section describes the devices used in the wireless sensor network (WSN) deployed, the measurement areas, and the dataset organization.

2.1. Acquisition Devices

Twelve temperature and humidity sensors, Xiaomi Mijia model LYWSDCGQ/01ZM, were used for data acquisition. These BLE devices are powered by an AAA battery that can last up to one year, according to the specifications of the manufacturer. The devices were calibrated in a Metrology Laboratory of the ITM accredited by the National Accreditation Body of Colombia (Organismo Nacional de Acreditación de Colombia—ONAC). The sensors calibration was performed using a Fluke 2626-H sensor as a reference measurement instrument. The environmental conditions under which the calibration was performed are between 19.30 °C and 20.50 °C for the temperature and between 56.4%RH and 60.5%RH for the relative humidity. The calibration range for temperature is from 15° to 40° and for relative humidity from 30%RH to 70%RH. The calibration summary of the temperature sensors is shown in Table 1 and the calibration summary of the relative humidity sensors is shown in Table 2.

The data from the twelve sensors are collected using a LoPy4 development board as BLE gateway. Each sensor reports the measurements, and the values are read by the LoPy4. The values of timestamp, temperature in °C, and relative humidity in %RH are added in a new line of the corresponding file, separated by comma. There is one file for each of the sensors and all twelve files are stored on the SD card of the development board. The general diagram of the deployed network is shown in Figure 1.

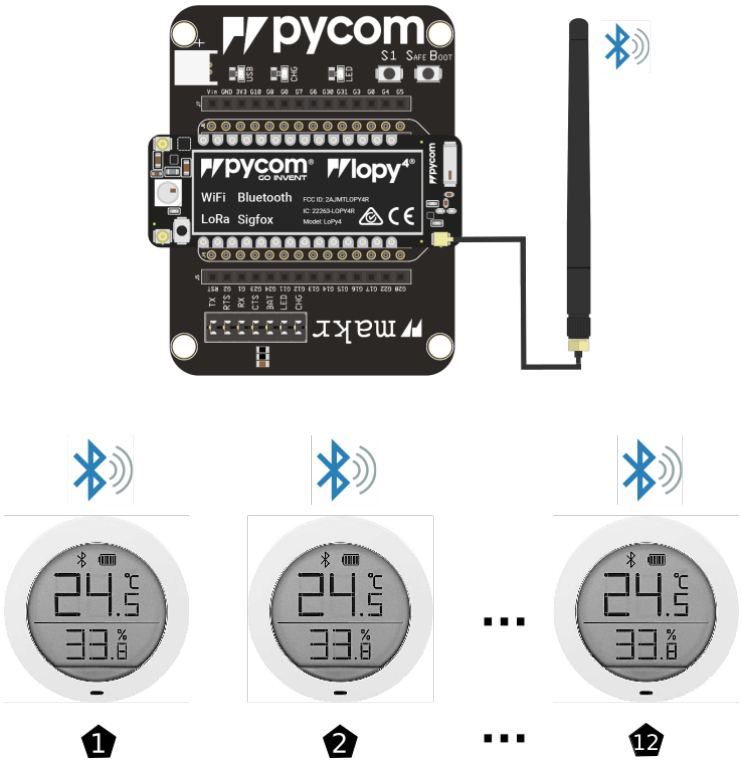

Figure 1. General diagram of the deployed network.

Table 1. Calibration summary of the temperature sensors.

ID	Control	Standard Indication [°C]	Sensor Measurement [°C]	Correction [°C]	Coverage Factor k	Expanded Uncertainty [°C]
1	15	15.30	15.45	−0.15	2	±0.49
1	20	20.03	20.00	0.03	2	±0.49
1	30	29.59	29.45	0.14	2	±0.49
1	40	38.75	37.85	0.90	2	±0.78
2	15	15.30	15.60	−0.30	2	±0.49
2	20	20.03	20.00	0.03	2	±0.49
2	30	29.59	29.35	0.24	2	±0.49
2	40	38.75	37.75	1.00	2	±0.77
3	15	15.30	15.45	−0.15	2	±0.49
3	20	20.03	19.90	0.13	2	±0.49
3	30	29.59	29.25	0.34	2	±0.49
3	40	38.75	37.50	1.25	2	±0.76
4	15	15.30	15.35	−0.05	2	±0.49
4	20	20.03	19.90	0.13	2	±0.49
4	30	29.59	29.70	−0.11	2	±0.49
4	40	38.75	38.45	0.30	2	±0.77
5	15	15.30	15.35	−0.05	2	±0.49
5	20	20.03	20.00	0.03	2	±0.49
5	30	29.59	29.70	−0.11	2	±0.49
5	40	38.75	38.30	0.45	2	±0.76
6	15	15.30	15.35	−0.05	2	±0.49
6	20	20.03	19.95	0.08	2	±0.49
6	30	29.59	29.55	0.04	2	±0.49
6	40	38.75	38.30	0.45	2	±0.77
7	15	15.30	15.50	−0.20	2	±0.49
7	20	20.03	20.10	−0.07	2	±0.49
7	30	29.59	29.50	0.09	2	±0.49
7	40	38.75	38.40	0.35	2	±0.76
8	15	15.30	15.55	−0.25	2	±0.49
8	20	20.03	20.10	−0.07	2	±0.49
8	30	29.59	29.50	0.09	2	±0.49
8	40	38.75	38.55	0.20	2	±0.76
9	15	15.30	15.30	0.00	2	±0.49
9	20	20.03	19.90	0.13	2	±0.49
9	30	29.59	29.35	0.24	2	±0.49
9	40	38.75	38.55	0.20	2	±0.76
10	15	15.30	14.85	0.45	2	±0.49
10	20	20.03	19.60	0.43	2	±0.49
10	30	29.59	29.30	0.29	2	±0.49
10	40	38.75	39.10	−0.35	2	±0.76
11	15	15.30	14.85	0.45	2	±0.49
11	20	20.03	19.70	0.33	2	±0.49
11	30	29.59	29.45	0.14	2	±0.49
11	40	38.75	39.45	−0.70	2	±0.76
12	15	15.30	14.70	0.60	2	±0.49
12	20	20.03	19.70	0.33	2	±0.49
12	30	29.59	29.45	0.14	2	±0.49
12	40	38.75	39.25	−0.50	2	±0.77

Table 2. Calibration summary of the relative humidity sensors.

ID	Control	Standard Indication [%HR]	Sensor Measurement [%HR]	Correction [%HR]	Coverage Factor k	Expanded Uncertainty [%HR]
1	30	30.3	32.3	−2.0	2	±1.6
1	50	49.7	52.1	−2.4	2	±2.5
1	60	59.7	61.5	−1.8	2	±2.1
1	70	69.8	70.8	−1.0	2	±2.3
2	30	30.3	33.8	−3.5	2	±1.6
2	50	49.7	53.4	−3.7	2	±2.5
2	60	59.7	62.5	−2.8	2	±2.1
2	70	69.8	71.1	−1.3	2	±2.3
3	30	30.3	32.4	−2.1	2	±1.6
3	50	49.7	52.4	−2.7	2	±2.5
3	60	59.7	61.6	−1.9	2	±2.1
3	70	69.8	71.0	−1.2	2	±2.3
4	30	30.3	34.3	−4.0	2	±1.6
4	50	49.7	53.3	−3.6	2	±2.5
4	60	59.7	62.3	−2.6	2	±2.1
4	70	69.8	71.2	−1.4	2	±2.3
5	30	30.3	34.3	−4.0	2	±1.6
5	50	49.7	53.7	−4.0	2	±2.5
5	60	59.7	62.9	−3.2	2	±2.1
5	70	69.8	71.4	−1.6	2	±2.3
6	30	30.3	31.8	−1.5	2	±1.6
6	50	49.7	51.8	−2.1	2	±2.5
6	60	59.7	61.0	−1.3	2	±2.1
6	70	69.8	70.4	−0.6	2	±2.3
7	30	30.3	34.1	−3.8	2	±1.6
7	50	49.7	53.6	−3.9	2	±2.5
7	60	59.7	62.6	−2.9	2	±2.1
7	70	69.8	71.8	−2.0	2	±2.3
8	30	30.3	32.1	−1.8	2	±1.6
8	50	49.7	51.9	−2.2	2	±2.5
8	60	59.7	61.5	−1.8	2	±2.1
8	70	69.8	70.7	−0.9	2	±2.3
9	30	30.3	32.2	−1.9	2	±1.6
9	50	49.7	52.4	−2.7	2	±2.5
9	60	59.7	61.4	−1.7	2	±2.1
9	70	69.8	71.6	−1.8	2	±2.3
10	30	30.3	32.8	−2.5	2	±1.7
10	50	49.7	52.6	−2.9	2	±2.6
10	60	59.7	62.1	−2.4	2	±2.1
10	70	69.8	70.7	−0.9	2	±2.3
11	30	30.3	32.6	−2.3	2	±1.6
11	50	49.7	52.2	−2.5	2	±2.5
11	60	59.7	61.6	−1.9	2	±2.1
11	70	69.8	70.3	−0.5	2	±2.3
12	30	30.3	32.4	−2.1	2	±1.6
12	50	49.7	52.3	−2.6	2	±2.5
12	60	59.7	62.0	−2.3	2	±2.1
12	70	69.8	70.7	−0.9	2	±2.3

2.2. Description of the Measurement Areas

The laboratory of Control Systems and Robotics of the Instituto Tecnológico Metropolitano size is 1350 cm by 620 cm. It has a single entrance, which is not airtight and is made of tempered glass. The room is distributed in two zones separated by a door in tempered glass and a division formed by a drywall in the lower part and tempered glass in the upper part. In the larger area are the workplaces and in the smaller area mainly the laboratory

equipment. The air conditioning system has three branches, two of which have their outlet in the area of workplaces and the other in the area of equipment. The air conditioning control system is located in a technical room adjacent to the laboratory, for which the access door is located outside the laboratory. The control system is configured with a temperature set point ranging between 18 °C and 20 °C.

The deployed network is distributed in nine nodes inside the laboratory, near the workstations, and three nodes outside the laboratory. One of the external nodes are in the technical room and two are in the hallway. The distribution of the sensors is shown in Figure 2. The external nodes were placed in order to have a reference of the temperature of the technical room and ambient temperature of the external area of the laboratory.

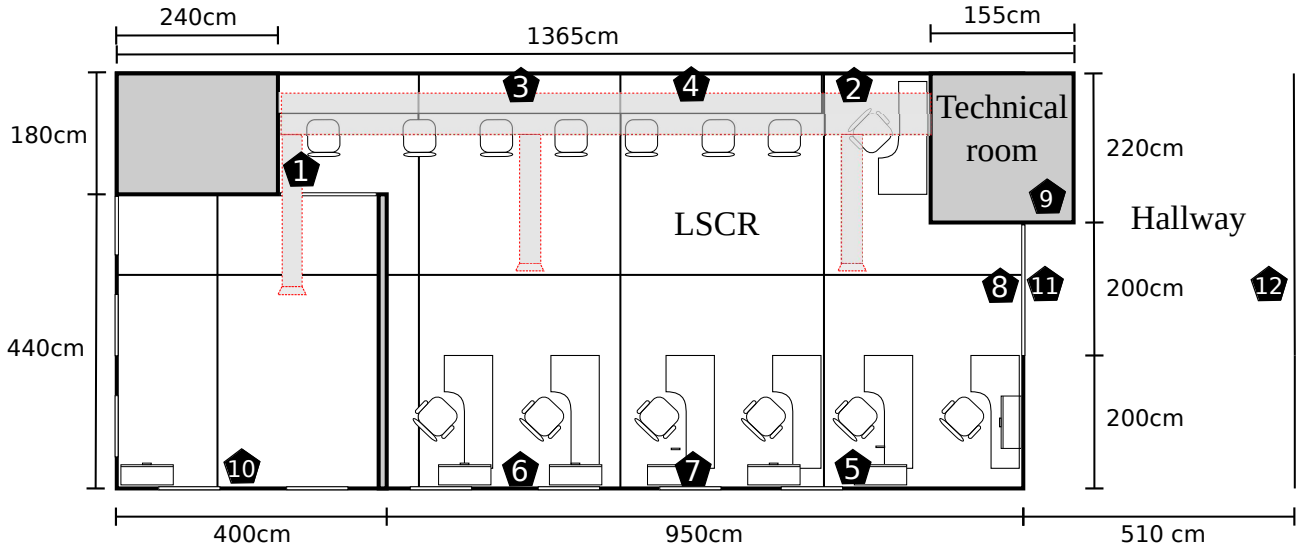

Figure 2. Floor plan with the distribution of the sensors at the laboratory of Control Systems and Robotics of the Instituto Tecnológico Metropolitano.

The De La Salle Museum of Natural Sciences was founded in 1913 by the De La Salle Brothers. It is committed to preserving, researching, and disseminating the cultural and natural heritage of the Antioquia region in Colombia. The zoological collection consists of 18,955 specimens, including amphibians and reptiles, birds, insects, crustaceans and arachnids, mammals, shells and molluscs, microorganisms, fish, and invertebrates. The anthropological collection contains elements that are more than 500 years old, made up of pre-Hispanic ceramics with a total of 383 pieces. Additionally, the museum has 89 ethnographic objects ranging from ceremonial costumes to bows, arrows, and distinctive clothing of different indigenous cultures in Colombia. Other collections in the museum include geology (2504 pieces), palaeontology (1009 pieces), history (89 historical objects), and botany (644 specimens).

The museum keeps the specimens and pieces of the collections that are not on exhibition in a storage room with controlled temperature and humidity. The room has a size of 1000 cm $\times$ 1600 cm and is full of cabinets for the storage of the specimens. There are cabinets placed along the walls and a larger one in the center of the room. In the latter, sensors were placed at the top and inside the cabinet (ID 1, 2, 3). The ID 12 sensor was placed outside the room in an environment without temperature and humidity control. The room has a humidifier where the ID 11 sensor is located and has air conditioning inlets on the wall next to the ID 7 and 8 sensors (see Figure 3).

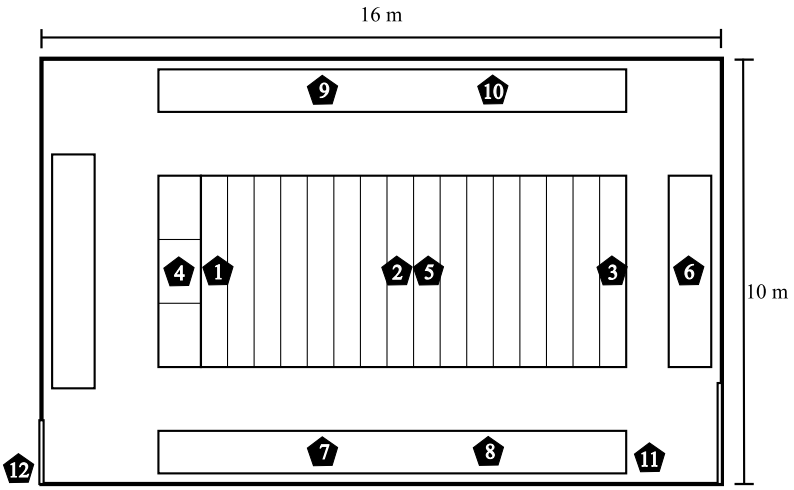

Figure 3. Floor plan with the distribution of the sensors at the storage room of De La Salle Museum of Natural Sciences of the Instituto Tecnológico Metropolitano.

2.3. Description of the Dataset Organization

The dataset consists of a total of 4,164,267 values. The data are organized in two folders named October and November, according to the month in which the data were acquired. The data were collected under everyday operating conditions, at the laboratory from 1 to 31 October 2019, and at the museum from 1 to 30 November 2019. Each folder contains twelve files in text format, corresponding to each sensor. Each file contains an average of approximately 58,300 values of each variable. In the files, the first column corresponds to the timestamp, the next column corresponds to the relative humidity measurements, and the last column corresponds to the temperature measurements. The values in the rows are separated by commas. The dataset is available in Mendeley Data repository, and can be downloaded in a 17 MB ZIP file from [37].

The dataset files information is presented in Table 3. The sensor ID allows to identify the location of the sensors according to the distributions shown in Figures 2 and 3. The MAC addresses of the sensors are shown in the second column. The filename of the file associated with each sensor is shown in the third column and it corresponds to the MAC address with the pairs of digits ordered in reverse order.

Table 3. ID, MAC, and filename of each sensor.

ID	*MAC-MJ_HT_V*1	Filename
1	58:2D:34:32:3C:EA	ea3c32342d58
2	4C:65:A8:DA:08:16	1608daa8654c
3	58:2D:34:32:3C:97	973c32342d58
4	4C:65:A8:DA:07:AC	ac07daa8654c
5	4C:65:A8:DA:08:46	4608daa8654c
6	58:2D:34:32:3C:BB	bb3c32342d58
7	4C:65:A8:DA:08:2E	2e08daa8654c
8	58:2D:34:32:41:23	234132342d58
9	58:2D:34:36:17:4D	4d1736342d58
10	58:2D:34:36:18:E6	e61836342d58
11	58:2D:34:36:16:D4	d41636342d58
12	58:2D:34:36:14:D6	d61436342d58

3. Temperature and Relative Humidity Dataset

This section presents some aspects related to the sampling and the analysis of some examples of the data acquired on specific dates in the laboratory and the museum.

3.1. Sampling Times

The acquisition system used in this work, which resembles the commercial acquisition methodology, presents physical challenges due to changes in the propagation medium of the signals that are common in real applications. For this reason, the dataset is also useful for the development of processing algorithms at the edge or post-processing, to mitigate some of these drawbacks derived, as we said, from electromagnetic propagation problems and connected with the use of sensors and low-cost systems that make the applications economically achievable. Given the above acquisition conditions, there is no defined sampling period for the acquisition performed. Sampling times can be obtained from the timestamp information of the collected data. In order to provide more information about the sampling, Figure 4 shows histograms, taking as reference the sampling time for each of the sensors in the November measurement. Ninety-nine percent of the sampling times were ordered from lowest to highest value to eliminate outliers corresponding to high sampling times. The red line shows the fit to a Weibull function, where it is observed that the reliability of the sampling time is clustered in the lower part of the distribution.

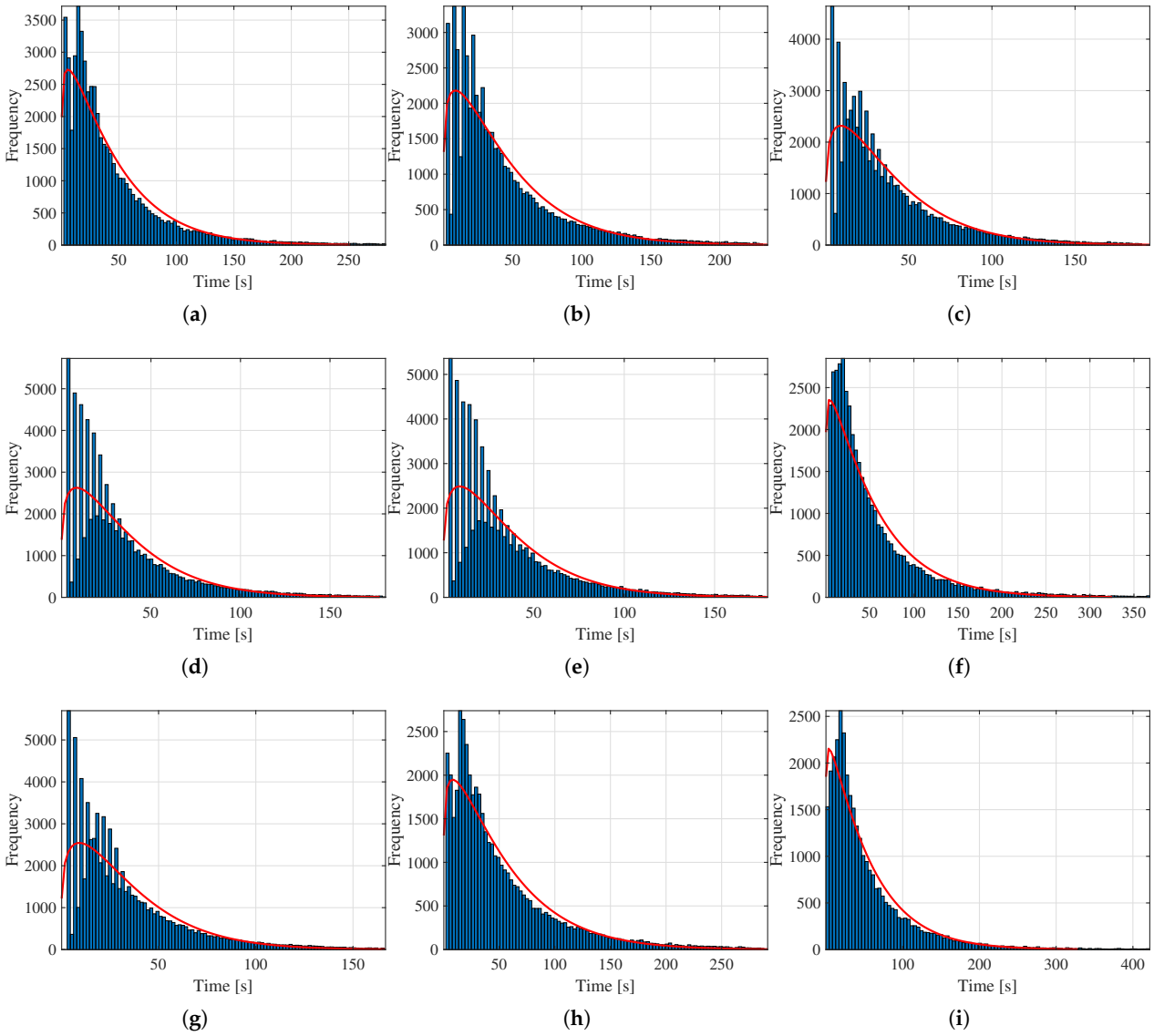

Figure 4. *Cont.*

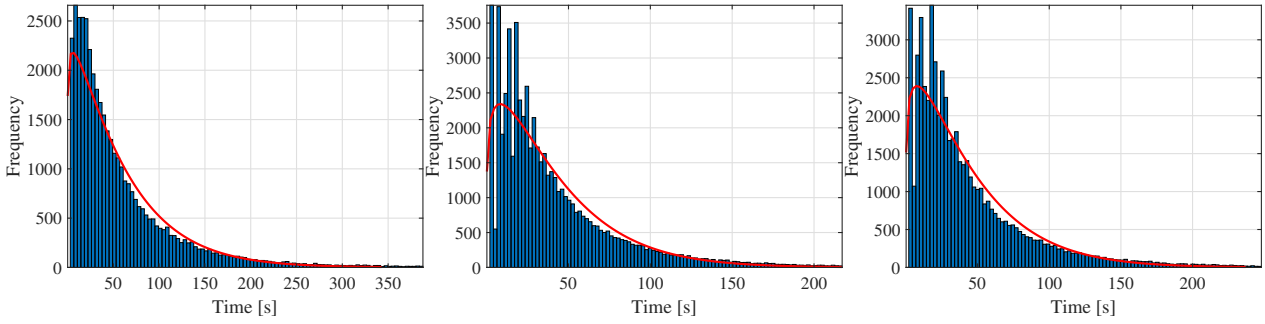

Figure 4. Histograms of the sampling time of the sensors. The red line shows the fit of the data to a Weibull distribution with 99% confidence interval. Sensor ID: (**a**) 1, (**b**) 2, (**c**) 3, (**d**) 4, (**e**) 5, (**f**) 6, (**g**) 7, (**h**) 8, (**i**) 9, (**j**) 10, (**k**) 11, and (**l**) 12.

The general description of the sampling times of the sensors is shown in Table 4. For the sensor network deployed in the museum storage room, some very high $t_{s_{max}}$ values are presented. However, from the histograms in Figure 4 and the $t_{s_{mean}}$ column, it is inferred that these values occurred rarely.

Table 4. Sampling features of the dataset: number of samples (NS), minimum sampling time ($t_{s_{min}}$), the maximum sampling time ($t_{s_{max}}$), and the average sampling time ($t_{s_{mean}}$).

ID	LSCR				Museum			
	NS	$t_{s_{min}}$ [ms]	$t_{s_{max}}$ [ms]	$t_{s_{mean}}$ [ms]	NS	$t_{s_{min}}$ [ms]	$t_{s_{max}}$ [ms]	$t_{s_{mean}}$ [ms]
1	56,679	3133	746,917	47,199	57,854	3116	1,198,834	46,267
2	59,385	3126	623,010	45,050	56,019	3129	1,798,383	47,766
3	58,519	3101	618,195	45,718	42,931	3151	62,836,468	60,775
4	60,707	3162	638,357	44,070	75,982	3128	763,660	35,228
5	61,802	3144	688,769	43,289	73,195	3083	1,226,431	36,574
6	55,462	2451	725,660	48,236	48,053	3158	1,250,817	55,705
7	58,147	3160	698,166	46,009	67,127	3070	639,113	39,876
8	62,730	3139	643,523	42,648	57,893	3100	720,683	46,237
9	60,256	3077	782,862	44,399	72,080	3105	603,800	37,140
10	54,308	3117	669,049	49,263	62,108	3117	678,896	43,094
11	56,976	3134	685,116	46,957	33,267	3140	83,725,641	77,941
12	55,194	3053	844,396	48,472	41,415	3157	4,635,723	64,555

3.2. Examples of Temperature and Humidity Data

The analysis of some examples of the data acquired on specific dates in the laboratory and the museum is presented below. In Figure 5, the plots of temperature data acquired on 2 October in the laboratory are shown. It is shown that during most of the day the sensors located inside the laboratory have a similar behavior. However, some sensors have close values depending on the area of the laboratory in which they are located. In addition, when there is an abrupt change in the temperature, all sensors report a close value. These changes generally occur when the air conditioning system is turned on or off.

Sensors with ID 1 and 10 generally indicate the lowest temperature values. The sensors with ID 2, 3, and 4 show very close values in the morning. In the afternoon, sensor 2 has a value of approximately one degree below sensors 3 and 4. Finally, in the evening, sensor 4 indicates a value higher than 1 degree above sensors 2 and 3. These sensors show values that are slightly above sensors 1 and 10. Sensors with ID 5, 6, and 7 show close values for the whole day, which are usually higher than the values of sensors 2, 3, and 4. The sensor with ID 8 shows the highest temperatures in the morning and the evening, which makes sense because it is located 80 cm higher than the other sensors. It should also be noted

that this sensor is located above the laboratory access door. Of the sensors external to the laboratory, the sensors with ID 11 and 12 have a similar behavior and provide information on the ambient temperature. The sensor with ID 9 has the smallest temperature variation range and its value is the closest to the temperature set point.

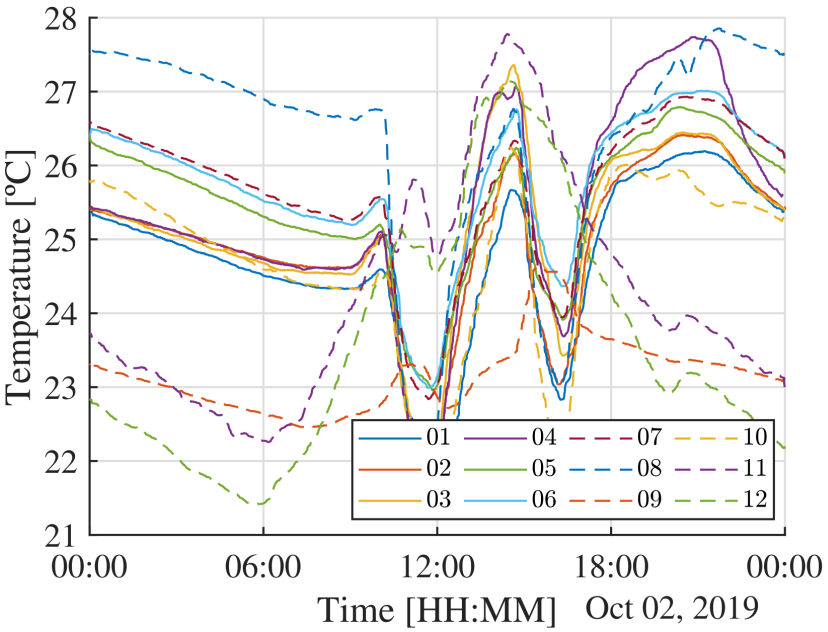

Figure 5. Temperature data acquired in the LSCR on 2 October.

In Figure 6, the plots of relative humidity data acquired on 2 October in the laboratory are shown. Although the inverse relationship between the two variables is evident, there are some differences in relation to the behavior of temperature. For example, the values indicated by sensor 6 in the morning are below the values of the other sensors located in the laboratory, which have values close to each other. A similar behavior is observed at night, with the difference in the slight increase of humidity indicated by sensor 10.

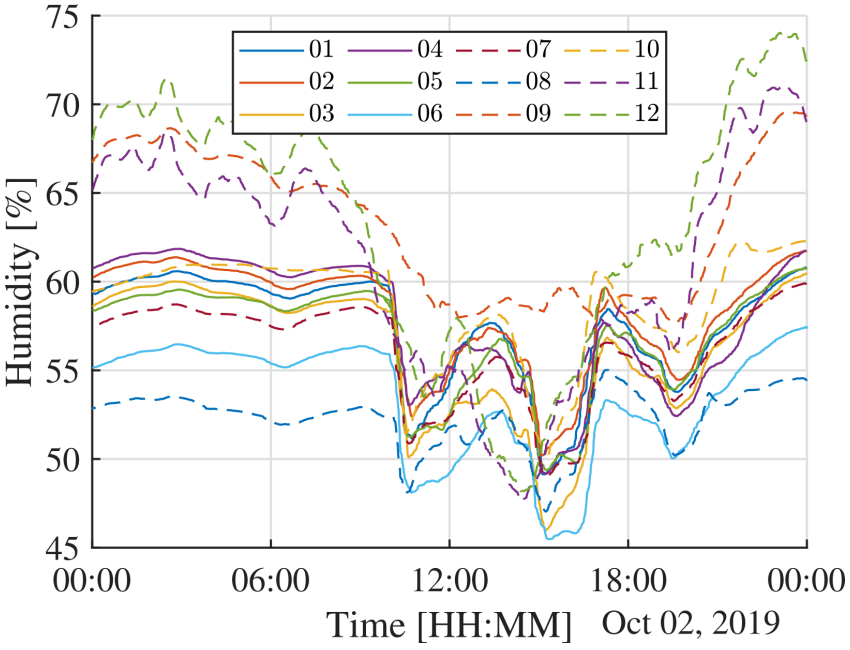

Figure 6. Relative humidity data acquired in the LSCR on 2 October.

In Figure 7, the plots of temperature data acquired on 20 October in the laboratory are shown. This date is a non-working day because it is a Sunday, and the air conditioning was off all day. It is observed that the temperature changes inside the laboratory are smooth. It is also observed that, except for sensor 8, the sensors in the laboratory present close values. Before 06:00 h and after 18:00 h, a significant relationship between sensor location and measured temperature can be observed. The behavior observed in Figure 5 for the sensors inside the laboratory is preserved, where sensors 10 and 1 show the lowest values, followed by sensors 2, 3, and 4. Then, with a slightly higher temperature value, are the sensors 5, 6, and, 7. Finally, sensor 8 shows the highest temperature values, close to 0.5 °C difference.

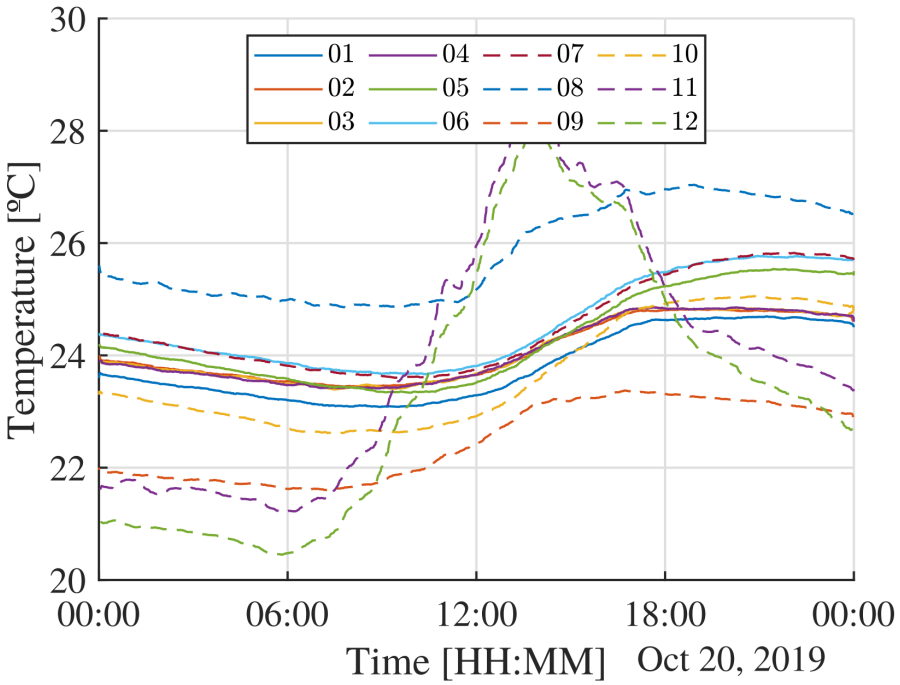

Figure 7. Temperature data acquired in the LSCR on 20 October.

In Figure 8, the plots of humidity data acquired on 20 October in the laboratory are shown. It is observed that the changes in the values of humidity inside the laboratory are smooth. Most of the sensors in the laboratory indicate close values of humidity, while sensor 6 reports values that are below the average of the other sensors. External sensors show a wider range of variation and more pronounced changes.

In Figure 9, the plots of temperature data acquired in the museum storage room on 20 November are shown. It is observed that the sensors with ID 1, 2, 3, and 5, which are located inside the central cabinet, present a similar behavior and with close values. The sensors with ID 4, 9, and 10, which are located above the cabinets, have a similar behavior, with sensor 4 having a value of approximately 0.5 degrees less than the other two sensors. The sensors with ID 7 and 8, which are located above the cabinets and near the air conditioning system outlet, indicate the lowest values. In most cases, we observed the relationship between the temperature measurements with the temperature changes indicated by the sensor with ID 12, which is located outside at the entrance of the storage room. The sensors with ID 6 and 11 indicate the values with the smallest variation.

In Figure 10, the plots of humidity data acquired in the museum storage room on 20 November are shown. It is observed that there is a greater variation in the measurements provided by the sensors during the first 9 h of the day. Similar behavior is observed at the end of the day. The measurements of sensor 11 show a different behavior from the other sensors, although their values are close.

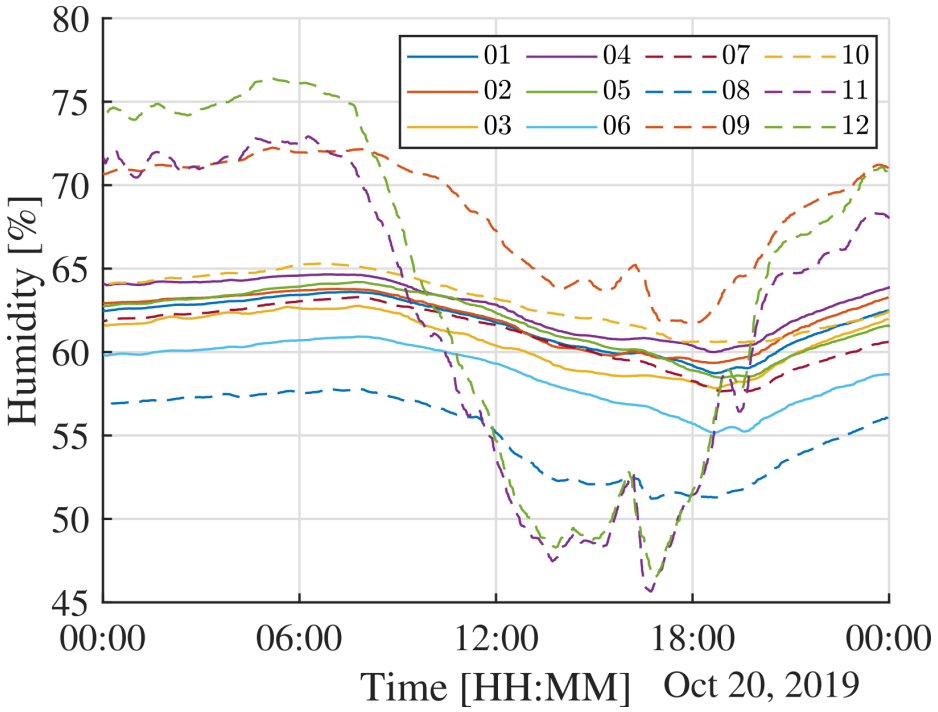

Figure 8. Relative humidity data acquired in the LSCR on 20 October.

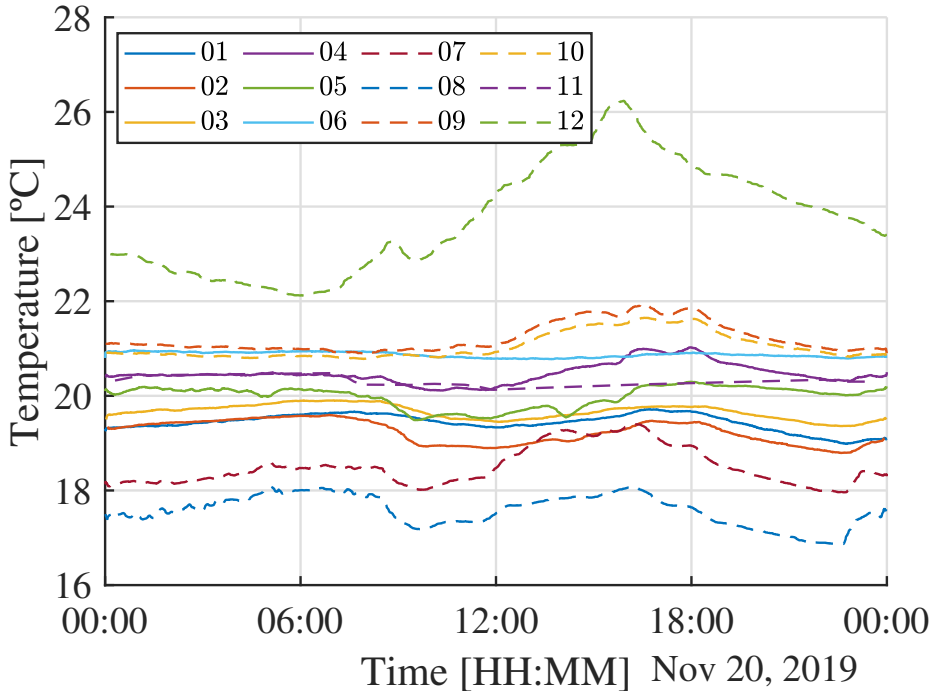

Figure 9. Temperature data acquired in the museum storage room on 20 November.

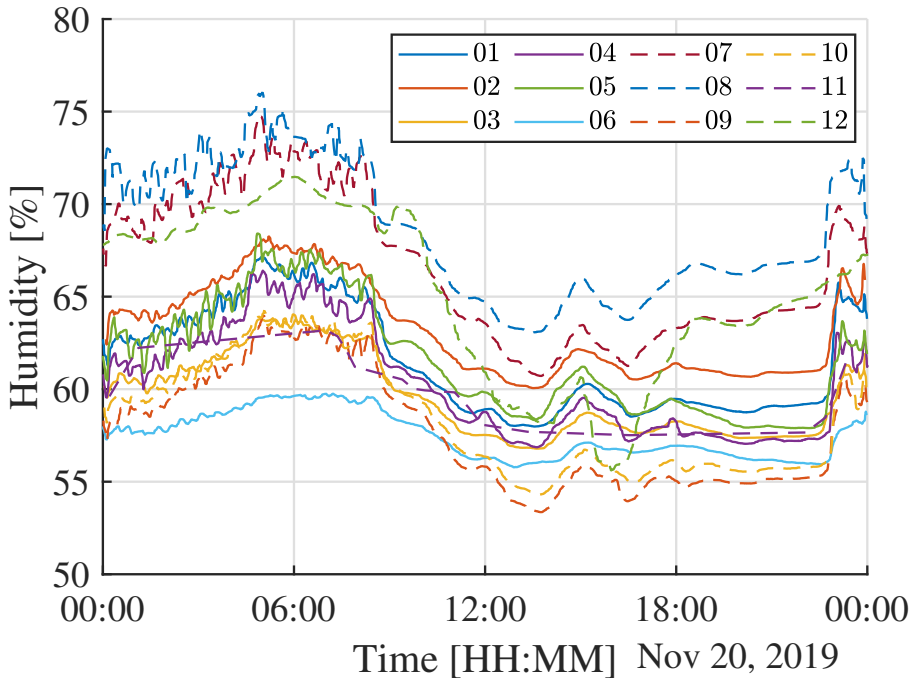

Figure 10. Relative humidity data acquired in the museum storage room on 20 November.

4. Conclusions

In this paper, the description of a dataset with the measurements of indoor temperature and relative humidity, acquired for two months with twelve Xiaomi Mijia sensors at the Instituto Tecnológico Metropolitano, Medellín—Colombia, is presented. The WSN deployed in this work for data acquisition presents physical challenges due to changes in the propagation medium of the signals that are common in real applications. For this reason, the dataset is useful for IoT researchers to develop processing algorithms at the edge or post-processing, to mitigate some of these drawbacks derived. In addition, data acquisition can be time-consuming, and having data to serve as a basis for researchers interested in digital signal processing and machine learning saves them from deploying sensor networks and focusing on algorithms implementation and evaluation. This dataset provides the timestamp, the measured variables, and floor plans with the sensors distribution of the deployed WSN. The data description presented in this article provides information about the sensors, the deployed sensor network, and the sampling, which can be useful for the use and analysis of the data.

Author Contributions: Conceptualization, J.B.-V., L.C.-L. and D.M.-V.; methodology, J.B.-V., L.C.-L. and D.M.-V.; validation, J.B.-V., L.C.-L. and D.M.-V.; writing—original draft preparation, J.B.-V., L.C.-L. and D.M.-V.; writing—review and editing, J.B.-V., L.C.-L. and D.M.-V.; funding acquisition, J.B.-V., L.C.-L. and D.M.-V. All authors have read and agreed to the published version of the manuscript.

Funding: The APC was funded by Instituto Tecnológico Metropolitano.

Institutional Review Board Statement: Not applicable.

Informed Consent Statement: Not applicable.

Data Availability Statement: Botero-Valencia, Juan; Castano-Londono, Luis; Marquez-Viloria, David (2022), "Indoor Temperature and Relative Humidity dataset", Mendeley Data, V1, doi: 10.17632/dxyvxk6h96.1.

Acknowledgments: This study was supported by the Automática, Electrónica y Ciencias Computacionales (AE&CC) Group COL0053581 and the Sistemas de Control y Robótica (GSCR) Group COL0123701, at the Sistemas de Control y Robótica Laboratory, attached to the Instituto Tecnológico Metropolitano.

Conflicts of Interest: The authors declare no conflict of interest.

References

1. Liu, Q.; Liu, W.; Sha, D.; Kumar, S.; Chang, E.; Arora, V.; Lan, H.; Li, Y.; Wang, Z.; Zhang, Y.; et al. An environmental data collection for COVID-19 pandemic research. *Data* **2020**, *5*, 68. [CrossRef]
2. Zhang, L.; Ji, H.; Huang, H.; Yi, N.; Shi, X.; Xie, S.; Li, Y.; Ye, Z.; Feng, P.; Lin, T.; et al. Wearable circuits sintered at room temperature directly on the skin surface for health monitoring. *ACS Appl. Mater. Interfaces* **2020**, *12*, 45504–45515. [CrossRef] [PubMed]
3. Marques, G.C.; von Seggern, F.; Dehm, S.; Breitung, B.; Hahn, H.; Dasgupta, S.; Tahoori, M.B.; Aghassi-Hagmann, J. Influence of humidity on the performance of composite polymer electrolyte-gated field-effect transistors and circuits. *IEEE Trans. Electron Devices* **2019**, *66*, 2202–2207. [CrossRef]
4. García, L.; Parra, L.; Jimenez, J.M.; Parra, M.; Lloret, J.; Mauri, P.V.; Lorenz, P. Deployment strategies of soil monitoring WSN for precision agriculture irrigation scheduling in rural areas. *Sensors* **2021**, *21*, 1693. [CrossRef]
5. Mylostyvyi, R.; Chernenko, O. Correlations between Environmental Factors and Milk Production of Holstein Cows. *Data* **2019**, *4*, 103. [CrossRef]
6. Gaur, A.; Lacasse, M.; Armstrong, M. Climate Data to Undertake Hygrothermal and Whole Building Simulations Under Projected Climate Change Influences for 11 Canadian Cities. *Data* **2019**, *4*, 72. [CrossRef]
7. Lai, D.; Liu, W.; Gan, T.; Liu, K.; Chen, Q. A review of mitigating strategies to improve the thermal environment and thermal comfort in urban outdoor spaces. *Sci. Total Environ.* **2019**, *661*, 337–353. [CrossRef]
8. Wolkoff, P. Indoor air humidity, air quality, and health–An overview. *Int. J. Hyg. Environ. Health* **2018**, *221*, 376–390. [CrossRef]
9. Tham, S.; Thompson, R.; Landeg, O.; Murray, K.A.; Waite, T. Indoor temperature and health: A global systematic review. *Public Health* **2020**, *179*, 9–17. [CrossRef]
10. Xu, X.; Zhong, Z.; Deng, S.; Zhang, X. A review on temperature and humidity control methods focusing on air-conditioning equipment and control algorithms applied in small-to-medium-sized buildings. *Energy Build.* **2018**, *162*, 163–176. [CrossRef]
11. Vela, A.; Alvarado-Uribe, J.; Ceballos, H.G. Indoor Environment Dataset to Estimate Room Occupancy. *Data* **2021**, *6*, 133. [CrossRef]
12. Monika, F.; Wargocki, P. Literature survey on how different factors influence human comfort in indoor environments. *Build. Environ.* **2011**, *46*, 922–937. [CrossRef]
13. Abhijeet, G.G.; Sinha, S.L.; Verma, T.N.; Dewangan, S.K. Investigation of indoor environment quality and factors affecting human comfort: A critical review. *Build. Environ.* **2021**, *204*, 108146. [CrossRef]
14. Kong, D.; Liu, H.; Wu, Y.; Li, B.; Wei, S.; Yuan, M. Effects of indoor humidity on building occupants' thermal comfort and evidence in terms of climate adaptation. *Build. Environ.* **2019**, *155*, 298–307. [CrossRef]
15. Jin, Y.; Wang, F.; Carpenter, M.; Weller, R.B.; Tabor, D.; Payne, S.R. The effect of indoor thermal and humidity condition on the oldest-old people's comfort and skin condition in winter. *Build. Environ.* **2020**, *174*, 106790. [CrossRef]
16. Marková, I.; Tureková, I.; Jad'ud'ová, J.; Hroncová, E. Analysis of Hygrothermal Microclimatic (HTM) Parameters in Specific Food Storage Environments in Slovakia. *Int. J. Environ. Res. Public Health* **2020**, *17*, 2092. [CrossRef]
17. Kramer, R.; Schellen, L.; Schellen, H. Adaptive temperature limits for air-conditioned museums in temperate climates. *Build. Res. Inf.* **2017**, *46*, 686–697. [CrossRef]
18. Kramer, R.P.; van Schijndel, A.W.M.; Schellen, H.L. The importance of integrally simulating the building, HVAC and control systems, and occupants' impact for energy predictions of buildings including temperature and humidity control: Validated case study museum Hermitage Amsterdam. *J. Build. Perform. Simul.* **2017**, *10*, 272–293. [CrossRef]
19. Magdalena, N.; Krzysztof, T.P. Conditions of the Internal Microclimate in the Museum. *J. Ecol. Eng.* **2020**, *21*, 205–209.
20. Yu, M.; Zhang, X.; Zhao, Y.; Zhang, X. A novel passive method for regulating both air temperature and relative humidity of the microenvironment in museum display cases. *Energies* **2019**, *12*, 3768. [CrossRef]
21. Shuang, X.; Dongyang, Z.; Zhen, L.; Hui, Z. A Combined Control Method of Temperature and Humidity Inside the Museum Cabinet. In Proceedings of the IEEE ICMTMA 2019, Qiqihar, China, 28–29 April 2019; pp. 322–326.
22. Sensor Data from Intel Berkeley Research Lab. Available online: http://db.csail.mit.edu/labdata/labdata.html (accessed on 6 May 2022).
23. He, J.; Li, Y.; Zhang, X.; Li, J. Missing and Corrupted Data Recovery in Wireless Sensor Networks Based on Weighted Robust Principal Component Analysis. *Sensors* **2022**, *22*, 1992. [CrossRef] [PubMed]
24. Hussein, M.K.; Marghescu, I.; Alduais, N.A. Performance of Data Reduction Algorithms for Wireless Sensor Network (WSN) using Different Real-Time Datasets: Analysis Study. *Int. J. Adv. Comput. Sci. Appl.* **2022**, *13*. [CrossRef]
25. Al-Shabi, M.; Abuhamdah, A. Using deep learning to detecting abnormal behavior in internet of things. *Int. J. Electr. Comput. Eng.* **2022**, *12*, 2088–8708. [CrossRef]
26. Esmaeili, H.; Bidgoli, B.M.; Hakami, V. CMML: Combined metaheuristic-machine learning for adaptable routing in clustered wireless sensor networks. *Appl. Soft Comput.* **2022**, *118*, 108477. [CrossRef]
27. Alghanmi, N.; Alotaibi, R.; Buhari, S.M. Machine Learning Approaches for Anomaly Detection in IoT: An Overview and Future Research Directions. *Wirel. Pers. Commun.* **2021**, *122*, 2309–2324. [CrossRef]

28. Dash, L.; Pattanayak, B.K.; Mishra, S.K.; Sahoo, K.S.; Jhanjhi, N.Z.; Baz, M.; Masud, M. A Data Aggregation Approach Exploiting Spatial and Temporal Correlation among Sensor Data in Wireless Sensor Networks. *Electronics* **2022**, *11*, 989. [CrossRef]
29. Ramadan, L.; Shahrour, I.; Mroueh, H.; Chehade, F.H. Use of Machine Learning Methods for Indoor Temperature Forecasting. *Future Internet* **2021**, *13*, 242. [CrossRef]
30. Attoue, N.; Shahrour, I.; Younes, R. Smart Building: Use of the Artificial Neural Network Approach for Indoor Temperature Forecasting. *Energies* **2018**, *11*, 395. [CrossRef]
31. Sadi, A.; Mera, D.; Fernández-Delgado, M.; Alkhabbas, F.; Olsson, C.M.; Davidsson, P. A comparison of machine learning algorithms for forecasting indoor temperature in smart buildings. In Proceedings of the 2018 4th International Conference on Computer and Information Sciences (ICCOINS), Kuala Lumpur, Malaysia, 13–14 August 2018; pp. 1–6. [CrossRef]
32. Baronti, P.; Barsocchi, P.; Chessa, S.; Mavilia, F.; Palumbo, F. Indoor Bluetooth Low Energy Dataset for Localization, Tracking, Occupancy, and Social Interaction. *Sensors* **2018**, *18*, 4462. [CrossRef]
33. Castillo-Atoche, A.; Vázquez-Castillo, J.; Osorio-De-La-Rosa, E.; Heredia-Lozano, J.C.; Viñas, J.A.; Cetina, R.Q.; Estrada-López, J.J. An energy-saving data statistics-driven management technique for bio-powered indoor wireless sensor nodes. *IEEE Trans. Instrum. Meas.* **2021**, *70*, 1–10. [CrossRef]
34. Longo, E.; Redondi, A.E.C.; Cesana, M. Accurate occupancy estimation with WiFi and bluetooth/BLE packet capture. *Comput. Netw.* **2019**, *163*, 106876. [CrossRef]
35. Krug, S.; O'Nils, M. Modeling and comparison of delay and energy cost of IoT data transfers. *IEEE Access* **2019**, *7*, 58654–58675. [CrossRef]
36. Rondón, R.; Mahmood, A.; Grimaldi, S.; Gidlund, M. Understanding the performance of bluetooth mesh: Reliability, delay, and scalability analysis. *IEEE Internet Things J.* **2019**, *7*, 2089–2101. [CrossRef]
37. Botero-Valencia, J.; Castano-Londono, L.; Marquez-Viloria, D. Indoor Temperature and Relative Humidity dataset. *Mendeley Data* **2022**, *V2*. [CrossRef]